Ocean Wave Energy Systems Design: Conceptual Design Methodology for the Operational Matching of the Wells Air Turbine

R. Curran[1]

Director of the Centre of Excellence for Integrated Aircraft Technologies (CEIAT), Reader, School of Mechanical and Aerospace Engineering, Queens University Belfast, NI, UK (Professor of Aerospace Management and Operations, TU Delft)

Abstract. The paper has set out a conceptual design methodology that was employed in the design of a Wells air turbine for OWC ocean wave energy plants. In particular, the operational matching of the performance of the turbine is used as the premise in achieving an optimal design configuration and sizing, given the range and frequency of power bands presented to the turbine over long periods of time. This is in contrast to designing the turbine to accommodate the average power rating delivered by the OWC. It was seen that this resulted in a 5% improvement in power output with the optimal size of the turbine required to be slightly larger than the average pneumatic power rating would suggest.

Keywords. Ocean wave energy, well turbine, design integration, concurrent engineering

1 Introduction

The paper sets out the conceptual design methodology that was employed in the design of a Wells air turbine for the OE Buoy prototype wave energy plant currently deployed in Galway Bay, Ireland. In particular, the operational matching of the performance of the turbine is used as the premise in achieving an optimal design configuration and sizing, given the range and frequency of power bands presented to the turbine over long periods of time. This is in contrast to designing the turbine to accommodate the average power rating delivered by the OWC, which ignores the wide range of power bands in which the turbine has to operate. The lowest and highest power bands can occur relatively frequently due to wave groupiness and also the hydraulic performance of the OWC influencing the occurrence profile, tending to result in negative turbine performance at the lower and higher ranges due to high running losses or separation and stall respectively.

In the study, the primary conversion from wave energy to kinetic energy is achieved with a floating Oscillating Water Column (OWC) of the 'backward bent

[1] Corresponding Author Email : r.curran@qub.ac.uk

duct' type, where the wave energy is used to excite vertical oscillations in the water column entrained in a floating plenum chamber with an open submerged base. The work was carried out to design a Wells turbine for this device that would ultimately couple to a generator set for power take-off. The prototype is currently deployed in Galway Bay Ireland.

It was decided that a Wells turbine configuration would used for the pneumatic power take-off as the most simple and robust turbine type that has been well tested in the field. It was evident for the pilot OC Buoy plant that a simple monoplane configuration would be most suitable. This provides a good efficiency rating across a sufficiently wide range of flow rates and can easily accommodate the power rating envisaged for the plant, not requiring a biplane configuration for example. Moreover, the monoplane design has a minimum of moving parts and therefore is robust and cheap to manufacture, for example as compared to a counter-rotating design. Other alternative turbine designs include the impulse turbine or the Dennis-Auld turbine. The impulse turbine has been well developed by the Japanese but does not offer significant gains due to its lower efficiency, although it is claimed to work across a wider range of flow rates, should that be required, at a lower rotational speed. The Dennis-Auld turbine is at an early stage of validation and is still under patent.

Since the conception of the Wells turbine [1] at Queen's University Belfast (QUB) there has been considerable effort devoted worldwide to the development of the basic design [2-8]. Similarly, there has been a considerable amount of development effort directed towards the self-rectifying impulse turbine that was first suggested by Kim et al. [9]. The development of the Wells turbine initially included investigations into the geometric variables, blade profile, and number of rotor planes [10], and also the use of guide vanes [11]. Two further design enhancements have been the pitching of a monoplane turbine's blades and the counter-rotation of a biplane's rotors [12]. Full scale plant systems [13] have utilized more advanced turbine configurations, encouraged by the successful pioneering of prototype plants such as the 75kW QUB Islay plant that utilized basic monoplane and biplane turbine configurations with standard symmetrical NACA profile blades [14, 15]. The development work for Impulse turbines also included investigation of the basic design parameters but much of the work then went on to focus on the design of the guide vanes and whether these would be fixed or pitching, or even self-pitching [16]. The Impulse turbine has been installed in several plants in Asia and there is still much interest in it as an alternative to the more widely used Wells turbine (used in plants in the UK, Portugal, India and Japan); while the Denniss-Auld turbine has been used in the Port Kembla Australian plant [17-19].

2 Input Pneumatic Power Data

The input data used to drive the design and sizing process was provided by the University of Cork. A distribution of estimated power conversion was gathered from the site in Galway Bay in order to provide the estimated pneumatic power

distribution. These figures are summarised below in Figure 2.1 in terms of a range of average pneumatic power in 2kW bands.

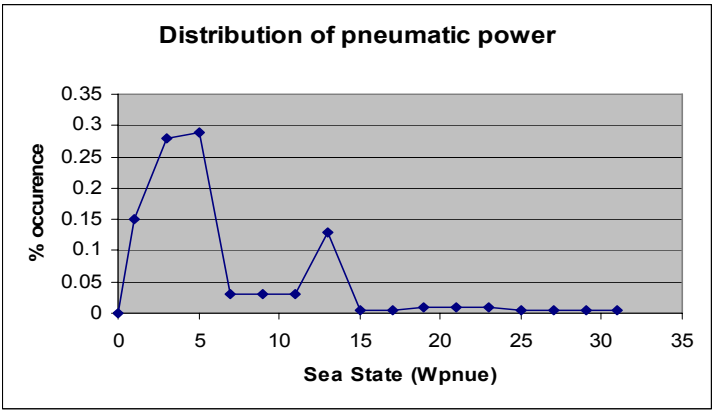

Figure 1. The input pneumatic power distribution for the OE Buoy

It can be seen that the maximum pneumatic power state was at 31kW and that there is a lot of irregularity in the range from 5-15kW. This may be due to hydrodynamic effects that occurring in Galway Bay where the input data was collected, being where the pilot plant will be deployed. However, the distribution may in practise be smoother if data from a much longer time scale was available, i.e. years rather than months. For the fullscale plant that will be next in the development for OceanEnergy, a more regular distribution would be expected in open sees. Not-with-standing the data was not smoothed and was used as provided.

A large amount of recorded instantaneous data wave height data was also provided by Cork University which showed that the summarised data presented in Figure 2.1 was actually averaging a significant amount of variation for each of the power states. It was evident that there was a very high occurrence of values around zero, a decreasing occurrence of values around the average and an increasingly low occurrence at values many times higher than the average. This is exemplified in Figure 2.2 which shows the distribution of pneumatic power recorded for a sea state with an average pneumatic power rating of 17kW. The power has been grouped according to occurrence in 2kW bins or increments, although the first bin is for values of less than 0.25kW, representing 16% of the occurring power bands. It can be seen that for that values as high as 155kW were recorded, approximately 9 times the average value of 17kW. It will be shown subsequently that never-the-less the turbine can be effectively designed for the seas where the there is the largest contribution of power. However, the irregular occurrence of such large pneumatic power surges will have to be accommodated in the plant. Although the turbine tends to be self limiting by stalling when driven beyond its design range, these power surges will cause large fluctuations in the turbine's axial loading and torque and it is expected that this will have a negative effect on the equipments survival. One very effective solution to this would be a blow-off valve which dumps excess power, as it is likely that a control strategy would not be able to react

fast enough by increasing the turbine rotational speed, this being a more gradual control strategy that is very effective over greater time periods. These irregular occurrences of very large pneumatic power spikes have not been noted as a feature of non-floating OWC devices and it is possible that the floating OE Buoy is displaying some unusual hydrodynamic effects, e.g. through extreme resonance, and this is an extra complication for the turbine and the general protection of the power take-off system.

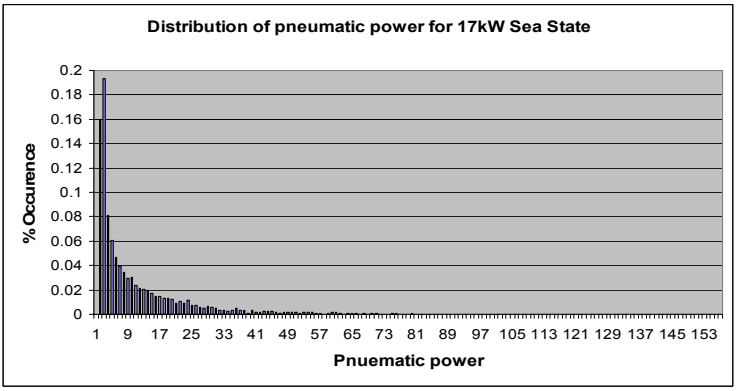

Figure 2. An example of the distribution of pneumatic power measured for the OE Buoy

Following on from some of the previous discussion, it is crucial to consider the actual contribution of power that is being provided by the sea states represented by Figure 2.2 for example. Therefore, Figure 2.3 presents the contribution of power available for the 17kW sea state presented in Figure 2.2. It will be evident from later presentation of the analysis that this tends to increase the size of the turbine, although it can be seen that there is negligible contribution at power levels of some 4 times the average value of 17kW.

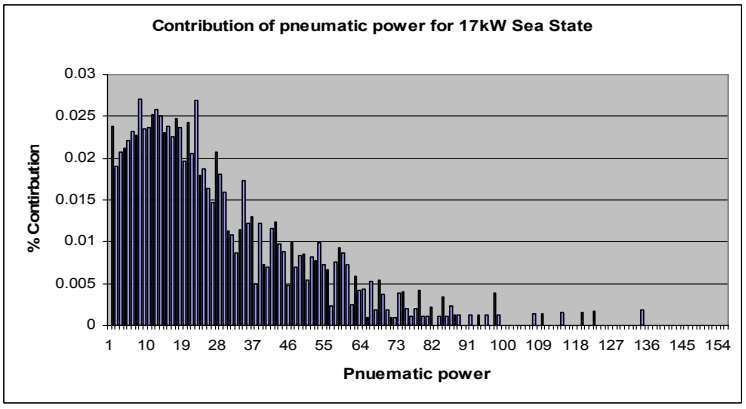

Figure 3. An example of the contribution of pneumatic power measured for the 17kW pneumatic power state

3 Turbine Design and Sizing Strategy

Initially, it was decided that the performance of the turbine should be individually assessed for each of the sea states represented in Figure 2.1 and that the design and sizing parameters would be chosen to maximise the overall rotational power output. However, it was then decided in consultation with Cork University that this "optimal" size should be decreased to ensure that the turbine would operate more efficiently in the smaller sea states, to increase running time rather than overall efficiency. Specifically, the result will be to reduce overall output but to increase running time and minimise time spent in shutdown, when the converted power would be less than the running losses.

It was pointed out in the previous section that the pneumatic power states presented in Figure 2.1 actually represent the average output from across a wide range of powers experienced during that associated "sea state". It is paramount that this global range is considered relative to the turbine's performance as the turbine has an effective range of flow rates across which it operates efficiently and these must therefore be matched over the long term. Consequently, there are two elements to the optimal matching: 1) globally matching the turbine's efficiency range to the range of pneumatic power states that maximises overall power conversion and 2) locally matching the turbine's efficiency range to the pneumatic power distribution associated with any particular pneumatic power range relating to a given sea state. However, as previously stated, the chosen turbine design was actually chosen to be smaller than the global optimal sizing value in order to increase running time.

In order to investigate the more detailed localised performance matching during each of the individual pneumatic power states, a generic distribution was used to generate the representative range of instantaneous pneumatic power values. Consequently, Figure 2.4 presents the general form of the distribution of pneumatic power, for example in terms of occurrence for the 5kW power state. It can be seen that relative to Figure 2.2 (noting that the x-axis is extended much further) the majority of occurrence is focused on the smaller powers but that there is a considerable occurrence of powers up to 3 times the average, in agreement with Figure 2.2, with much higher values also included in the analysis. Therefore, this is in qualitative agreement with the instantaneous distributions of wave height supplied by Cork University. The relevance of these higher values is that the turbine will have to be able to accommodate them, and will do so at a given value of efficiency determined by the turbine's efficiency characteristic. At the higher values of flow rate, relative to some nominal design point, the angle of attack onto the turbine blades approaches the stalling region at which point the efficiency drops considerable due to boundary layer separation and loss of lift. On the other hand, the lift at the lowest flow rates is not well developed due to the low angles of attack onto the blades and does not provide enough driving torque to overcome the running losses. This highlights the need for matching and the need to perform the analysis at this level of detail. Otherwise, the turbine might be sized more optimistically for the pneumatic power extremes while not being matched to the power bands that occur more, and which represent the majority of the input power.

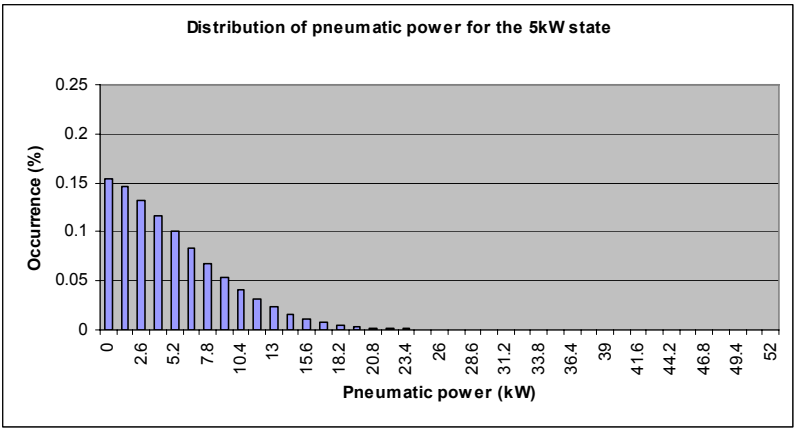

Figure 4. Example of power distribution associated with pneumatic power state

4. Performance Analysis

4.1 Air Turbine Performance

The turbine performance is driven by a number of key variables and parameters, including: V is the air velocity, Q is the airflow, T is torque, P is pressure, and Ω is rotational speed. The turbine performance is usually quoted in terms of non-dimensional equivalents of flow rate ϕ, pressure P^*, damping ratio B_R, torque T^*, and efficiency η are also included and are given by Equations 1 through 5 respectively.

$$\phi = \frac{V_A}{U_t},\ P^* = \frac{P}{\rho_A \omega^2 D_t^2},\ B_R = \frac{P^*}{\phi},\ T^* = \frac{T}{\rho_A \omega^2 D_t^5},\ \eta = \frac{T\omega}{PQ} \qquad (1\text{-}5)$$

where U_t is the rotational velocity, ρ_A is the density of air, ω is the angular velocity, and D_t is the rotor tip diameter. It is important to consider the non-dimensional characteristics as turbines of various values of geometry, speed and type can then be compared in absolute terms. It is known that the damping ratio B_R can be said to be linear for the majority of the flow range, apart from when in the stall region where secondary flow effects become more dominant. The linearity is an extremely important characteristic as the turbine can be simply designed to apply a constant level of applied damping to the OWC. This damping should maximise the output from the OWC while also producing the optimal range of airflow rates to maximise the turbine's conversion, as previously pointed out. In the analysis the turbine damping ratio is used to predict the airflow velocities produced by turbines of various sizes, given the range of pneumatic power states/outputs being considered

from the OWC, see Figure 2.1. The efficiencies corresponding to these velocities will then be used to give the conversion performance of the turbine.

It is worth pointing out that variable speed control could be considered for the plant so that the speed can be altered in steps of say 50rpm, in order to match the turbine optimally to the output of the OWC. This control technique has been previously utilised on the Islay LIMPET device for the Wells turbine where the speed is reduced in order to decrease the applied damping and therefore, increase the flow rate to a value that produces a higher efficiency.

The efficiency characteristic for the turbine was estimated from a synthesis of small-scale steady-state results and full-scale random oscillating flow measurements published for the Islay pilot plant. Much of the literature published on Wells turbine performance results tends to project performance enhancements at full scale, relative to laboratory results, due to the reduced drag associated with the increase Reynolds Numbers. However, it is the author's opinion that any potential increase in efficiency tends to be countered by the negative dynamic effects of accelerating oscillating flow. However, the damping ratio B_R provided by the turbine tends to be slightly higher and the effects of stall seem to be less acute than at small scale. These issues have been taken into account in formulating the instantaneous efficiency characteristic for the monoplane turbine to be used in the OE Buoy, which is required in matching the turbine performance to the individual pneumatic power states.

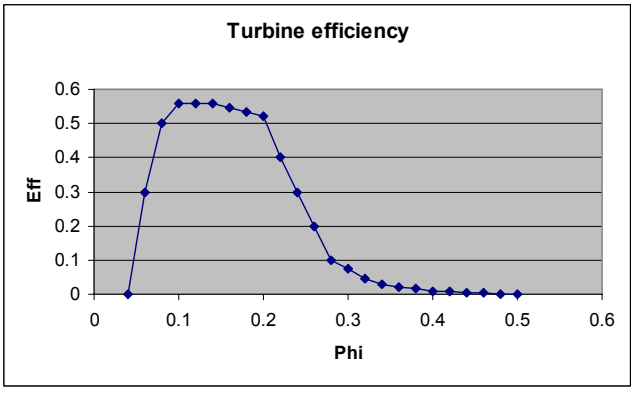

Figure 5. Non-dimensional efficiency for the OE Buoy monoplane Wells turbine

It can be seen from Figure 2.5 that the instantaneous turbine efficiency η (denoted by *Eff*) varies considerably with the flow rate ϕ (denoted by *Phi*). The running losses due to blade drag at zero flow result in a negative efficiency and at a flow coefficient of approximately 0.2 stall occurs progressively from the blade root towards the tip to give the turbine an effective flow range of approximately 0.04 - 0.3. It is readily evident and well illustrated now that this effective operational range, shown in Figure 2.5, needs to coincide with the occurrence of pneumatic power typified in Figure 2.4. The following Section establishes that this is achieved

through the level of damping ratio of the turbine which then provides the pneumatic power at the correct flow rates; the latter being associated with a range of angles of attack that are appropriate for the blades' aerofoil profile. The peak efficiency of just below 60% is conservative relative to more optimistic literature but correlates well to the authors work with full scale plants. Importantly, the estimation of the turbine efficiency characteristic has been conservative in order to not oversize the turbine, any increased conversion performance being easily accommodated by the electrical system.

4.2 OWC-Turbine Coupling and Power Conversion

Given that the output of the OWC has been estimated (Figure 2.1) along with the performance of the turbine (Figure 2.5), the two have to be coupled in order to calculate the final power output. Here, the damping applied by the turbine can be said to act as a gearing ratio, between the two, that determines the forced velocity of the airflow due to the action of the OWC. Therefore, the damping can be expressed as shown in Equation 6,

$$B_A = P\frac{A_C}{V_C} \tag{6}$$

while, assuming incompressibility of air and a Mach number of less than 0.5, and conservation of mass flow, Equation 6 can be further manipulated to give

$$B_A = P\frac{A_C^2}{A_A V_A} \tag{7}$$

where A_C and A_A are the cross-sectional areas at the water column surface and turbine duct respectively, and V_C and V_A are the respective air velocities. Finally, substituting in Equations 1 and 2, Equation 7 can be expressed in terms of the turbine's damping ratio B_R, as shown in Equation 8 below.

$$B_A = 4\rho_W\left(\frac{A_C^2}{A_A}\right)U_t\left(\frac{P^*}{\phi}\right) \tag{8}$$

It has been established that the effective damping ratio B_R, or pressure-flow ratio, of the constant-speed Wells turbine is constant. Consequently, the actual applied damping of the turbine can be calculated for any turbine geometry A_A and then substituted into Equation 7 to provide the pressure-velocity ratio. As the pneumatic power provided by the OWC is expressed by Eq. 9,

$$W_p = PV_A A_A \tag{9}$$

then Equations 7 and 9 can be combined to give Eq. 10.

$$V_A = \sqrt{\frac{W_p A_C^2}{B_A}} \tag{10}$$

Therefore, Equation 10 can be used to give the air velocity that corresponds to a particular value of pneumatic power. Equations 8 and 10 show that the geometry of the OWC and turbine, the rotational speed of the turbine and the damping ratio of

the turbine define the above relationship. Consequently, for the fixed-speed machine, it is a simple matter to take the air velocity and to find the efficiency relating to that value. Thereafter, the values of pneumatic power, given by the distributions represented by Figure 2.4, can be multiplied by the efficiency to give the final power output for that pneumatic power state, the summation of the energy output for all states considered in the distribution in Figure 2.1 giving the overall output of the plant.

5 Analysis Results

There were 16 pneumatic power states considered in the analysis, derived from Figure 2.1, with each state being described by a distribution of the form shown in Figure 2.4 (based on the form exemplified in Figure 2.2). Subsequently, the analysis considered the individual values of pneumatic power in order to determine the relevant turbine conversion performance associated with each sea state, the conversion being calculated for that pneumatic power state relative to the occurrence data typified in Figure 2.4. A final value for the power conversion across a given time period was then calculated given the occurrence data presented in Figure 2.1. This value of converted energy was the basis of the optimisation procedure, being the objective function to be maximised. However, as previously stated, this optimal design was adjusted to allow the turbine to operate in a greater percentage of the sea states, even although the overall energy output would be lower due to the reduced ability of the turbine to efficiently convert in the larger pneumatic power states that contain a significant proportion of the available pneumatic power.

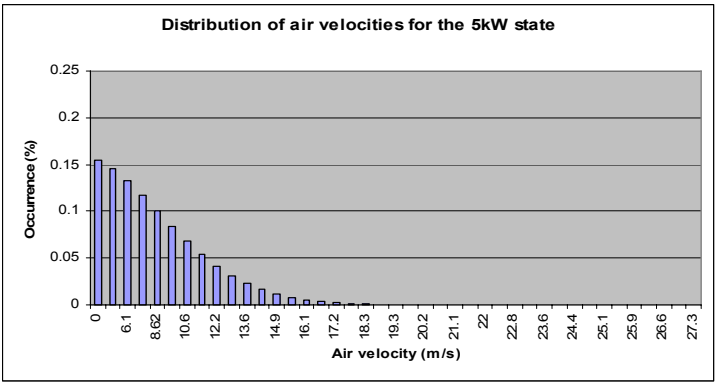

Figure 6. Example of air velocity distribution with pneumatic power state

The conversion of the pneumatic power to a flow rate at a given pressure drop was predicted according to the analysis presented in Section 2.4.2. Figure 2.6 presents the occurrence distribution of air velocities for the pneumatic power distribution presented in Figure 2.4. The predicted flow rate was then used to

determine the turbine performance, taken from the characteristic presented in Figure 2.5. The matching of the flow rate and the turbine efficiency is exemplified in Figure 2.7 relative to occurrence, showing the two plots superimposed in order to highlight that the turbine needs to be designed in order to accommodate flow range across its most efficient range but also to minimise the amount of time when running at negative efficiencies at the lowest flow rates.

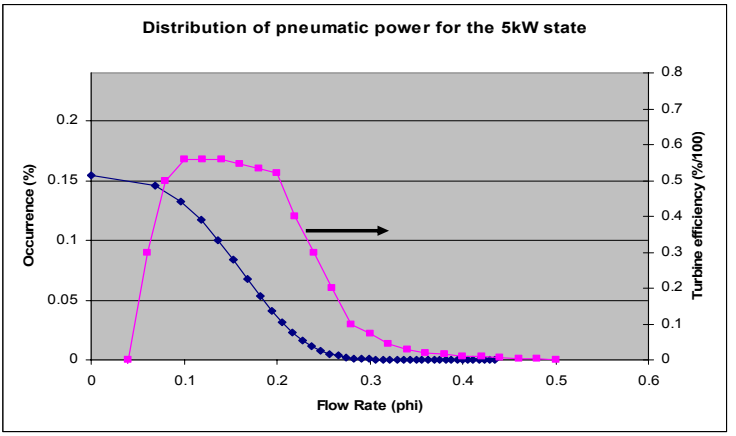

Figure 7. Example of matching the turbine performance to the pneumatic energy distribution

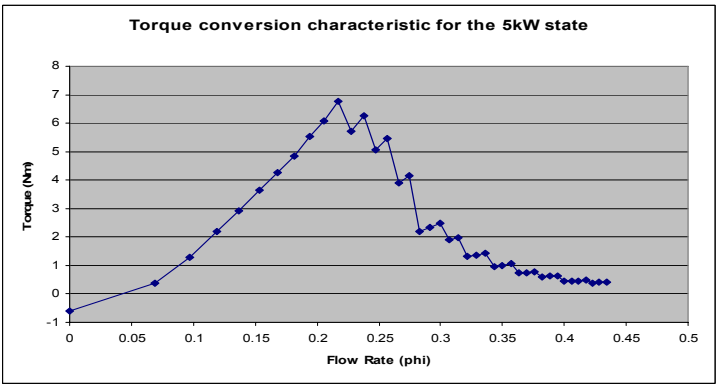

Figure 8. Example of torque conversion

Ultimately, the turbine performs with an associated efficiency and produces torque that is then used to drive an alternator for example. An example of the torque conversion for the pneumatic power state represented in the previous Figures is presented in Figure 2.8. It is important to note that the characteristic is not a distribution of torque but rather the instantaneous performance. In practise the zigzag profile at the stall region at phi values of over 0.2 would actually be smooth but appears as it does from the analysis due to the low fidelity of the data

points from the turbine efficiency curve, shown in Figure 2.7. It can also be seen that the turbine runs at a loss at the lowest values of flowrate due to the blade drag. However, it is evident that the torque performance relates well to the majority of flow rates occurring most regularly in Figure 2.7. Relative to Figures 2.2 and 2.3 in terms of the correlation of power contribution to power band occurrence, it is clear that the contribution of power will also tend to shift to the higher powers, thereby better utilising the toque conversion performance presented in Figure 2.8.

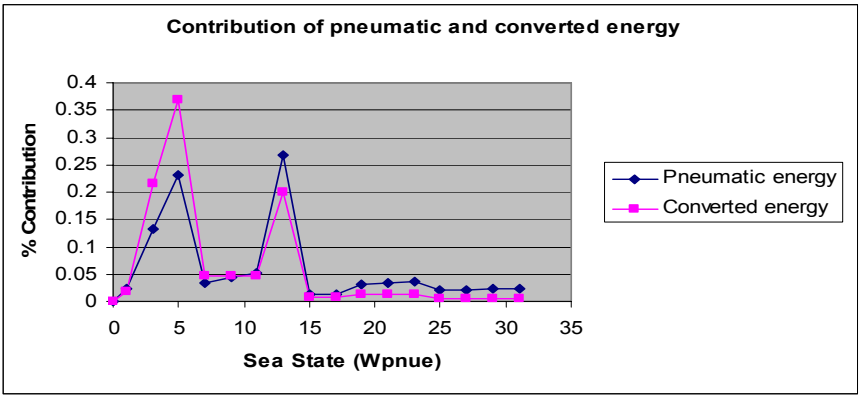

Figure 9. Distribution of pneumatic and converted power

Figure 2.9 shows a plot of the distribution of contributed converted power relative to the contributed pneumatic power (as opposed to occurrence shown in Figure 2.1). The energy levels relate to a nominal period of one year as it is the energy being converted over a period of time that should be used in the calculation of optimal conversion efficiency. However, it is important to note that the period for the analysis is not influential in the optimal sizing as the distribution shown in Figure 2.1 is assumed to be consistent and representative for any extended time period.

Figure 2.10 shows the distribution of associated conversion efficiencies from Figure 2.9, being the ratios of the compared pneumatic and converted power values. The Figure also plots the distribution of maximum torque values generated by the turbine. It is interesting to note the turbine's stalling phenomenon has tended to cap the torque rating of the system and acts as a natural form of limiting, the remainder of the energy at the highest flow rates being dissipated in separated and turbulent airflow. However, in practise there maybe a fatigue issue for the turbine over its life time due to these large oscillations in blade load, as the blades are experiencing catastrophic stall in the larger pneumatic power states. As noted in Section 2.2, this seems to be more extreme and potentially is a major design criteria for the OE Buoy.

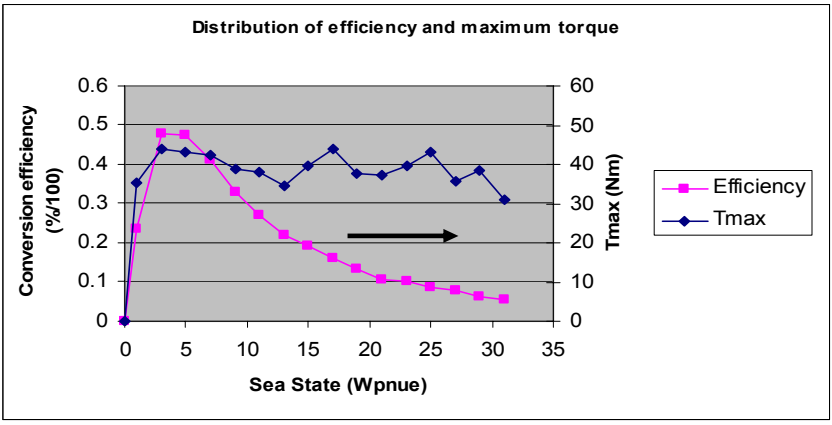

Figure 10. Distribution of overall conversion efficiency and the maximum torque values

The optimal efficiency of the turbine using the presented methodology was calculated to be 40% at a Radius of 0.48m, converting 21.7kWhr per annum. The average pneumatic power rating of 6.3kW was also used as an alternative optimal design point in order to show the benefit of taking the operational view to the optimisation process. The average pneumatic power method returned an optimal efficiency of 37.5% at a Radius of 0.45m, converting 20.7kWhr per annum. Interestingly, the 2.5% improvement in the performance efficiency of the turbine actually translates to a doubling of the actual output of 5% in terms of the converted output, i.e. a 5% increase in sales revenue. This is due to the turbine plant performing better over the whole range of pneumatic power bands accommodated by the turbine in actual terms, rather than relative to input power.

6 Final Design Parameters

The overall efficiency of the turbine is presented in Table 2. Also included is the relative values for the "optimal" turbine design that was altered in order to increase the amount of time when the system would be running efficiently, i.e. not at an overall loss. It can be seen that the nominal rotational speed has been kept fixed at 1500rpm, while the design of the electrical equipment is reported to allow considerable speed range. This will allow the speed to be reduced in the smaller seas in order to increase the flow rates so that the pneumatic power is delivered at values over which the turbine is more efficient. Obviously, this will increase the values of overall efficiency towards that of the optimal design but more importantly, will allow an effective speed control strategy to be put in place that will ensure increased efficient running time. Such a strategy is not in the remit of this report, especially without the electrical system design yet available.

Table 1. Basic design variables for analysis

Parameter	*Final design*	*"Optimal design"*
Tip radius (m)	0.4	0.4
Speed (rpm)	1500 (Fixed speed)	2100 (Fixed speed)
Damping *Ba* (Ns/m)	125,000	175,000
Overall efficiency	30%	40%

To enable the analysis a number of design parameters are input variables that will determined relative to the optimisation procedure while other input variables are fixed or absolute. These are shown in Table 2, notably including turbine tip diameter *Tdiameter*, the hub-to-tip ratio *H-T ratio*, the rotational speed *w (rad/sec)*, the turbine applied damping *Ba (Ns/m)* and the turbine's linear damping slope *P*/phi*.

Table 2. Input design variables for analysis

Variable	
w =	157.0796
Gravity=	9.81
Col lgth=	2
Rhub=	0.26383
RHOair =	1.225
Acol =	12
Rtip =	0.4
H-T ratio	0.659575
Aduct =	0.28398
RPM =	1500
Ut =	62.83185
Ba =	124893.6
P*/phi =	0.8
Ac/Ad =	42.25646
Col width	6
Annual hr=	8766
Tdiameter	0.8
Hdiameter	0.52766

In determining the turbine's linear damping slope *P*/phi*, there is an associated calculation to calculate the turbine's solidity (blade to annular area ratio) which in turn determines the correct value, from historical data. The solidity was determined to be 0.59.

7 Conclusions

The paper has set out a conceptual design methodology that was employed in the design of a Wells air turbine for OWC ocean wave energy plants. In particular, the operational matching of the performance of the turbine is used as the premise in achieving an optimal design configuration and sizing, given the range and frequency of power bands presented to the turbine over long periods of time. This is in contrast to designing the turbine to accommodate the average power rating delivered by the OWC. It was seen that this resulted in a 5% improvement in power output with the optimal size of the turbine required to be slightly larger than the average pneumatic power rating would suggest. However, it should be noted that the case study used in the paper had a very large distribution of powers at the higher values and that other geographical positions may result in a smaller turbine being better than the average pneumatic power rating would suggest. This highlights the benefit of such an operational oriented design methodology that allows the designer to tailor the sizing relative to the distribution of power rather than being confined to a single solution for a given average pneumatic power rating: the optimal sizing and configuration is also a function of the distribution, albeit to a lesser degree than the average pneumatic power rating.

8 References

[1] Wells, AA (1976), Fluid Driven Rotary Transducer, British Patent Spec. 1 595 700.

[2] Curran, R., and Gato, L.C. The energy conversion performance of several types of Wells turbine designs. Journal of Power and Energy, Proceedings of The IMechE, Part A, 1997, Vol. 211, No. A2, ISSN 0957-6509, pp 55-62.

[3] Curran, R, Whittaker, TJT, Raghunathan, S, and Beattie, WC (1998a). "Performance Prediction of the Counterrotating Wells Turbine for Wave Energy Converters, J Energy Engineering, ASCE, Vol. 124, pp. 35-53.

[4] Curran, R and M Folley, (Invited Book Chapter)" Integrated Air Turbine Design for Ocean Wave Energy Conversion Systems", Ocean Wave Power, Springer, submitted.

[5] Folley, M, Curran R, and T Whittaker, "Comparison of LIMPET contra-rotating wells turbine with theoretical and model test predictions", Ocean Engineering, Volume 33, Issues 8-9, June 2006, Pages 1056-1069.

[6] Count, B (1980). Power from Sea Waves, Academic Press, New York, ISBN 0-12-193550-7.

[7] Mei, C.C. Power extraction from water waves. Journal of Ship Research, 1976, Vol. 20, No. 2, pp. 63-66.

[8] Salter, Stephen, H, (1988). "World Progress in Wave Energy," Int J Ambient Energy, Vol 10, pp 3-24.

[9] Kim TW, Kaneko K, Setoguchi T and Inoue M. (1988). "Aerodynamic performance of an impulse turbine with self-pitch-controlled guide vanes for wave power generator", Proceedings of 1st KSME-JSME Thermal and Fluid Eng Conf, Vol. 2, pp133–137.

[10] Raghunathan, S (1995). "A Methodology for Wells Turbine Design for Wave Energy Conversion," J Power Energy, IMechE, Vol 209, pp 221-232.
[11] Setoguchi, T., Takao, M., Kaneko, K., 1998. Hysteresis on Wells turbine characteristics in reciprocating flow, International Journal of Rotating Machinery, vol. 4 (1), 17–24.
[12] Raghunathan, S, and Beattie, WC (1996). "Aerodynamic Performance of Counter-rotating Wells Turbine for Wave Energy Conversion," J Power Energy, Vol 210, pp 431-447.
[13] Falcao, AF, Whittaker, TJT, and Lewis, AW (1994). Joule 2, Preliminary Action: European Pilot Plant Study, European Commission Report, JOUR-CT912-0133, Science Research and Development-Joint Research Center.
[14] Whittaker, TJT, Beattie, WC, Raghunathan, S, Thompson, A, Stewart, T and Curran, R (1997). "The Islay Wave Power Project: an Engineering Perspective," Water Maritime and Energy, ICE, pp. 189-201.
[15] Whittaker, TJT, Thompson, A, Curran, R, Stewart, TP (1997), European Wave Energy Pilot Plant on Islay (UK), European Commission, Directorate General XII, Science, Research and Development - Joint Research Centre, JOU-CT94-0267.
[16] Setoguchi T, Santhakumar S, Maeda H, Takao M and Kaneko K (2001). "A review of impulse turbines for wave energy conversion", Renewable Energy, Vol. 23, pp 261–292.
[17] Curran, R. (2002). Renewabe Energy: Trends and Prospects, Chapter 6: Ocean Energy from Wave to Wire. Editors: Majumdar, SK, Miller, EW, and Panah, AI., The Pennsylvania Academy of Science, pp 86-121.
[18] Finnigan, T, and Auld, D, (2003). Model Testing of a Variable-Pitch Aerodynamic Turbine, Proc. 13th Int. Offshore Mechcnics and Arctic Engineering Conf, ISOPE, Vol 1, pp 357-360.
[19] Finnigan, T, and Alcorn, R, (2003). Numerical Simulation of a Variable Pitch Turbine with Spee Curran, R., Denniss, T., and Boake, C. (2000), Multidisciplinary Design for Performance: Ocean Wave Energy Conversion, Proc. ISOPE'2000, Seattle, USA, ISSN 1098-6189, pp. 434-441.